COMPARISON OF 1D AND 3D HYDRODYNAMIC MODELS IN DESIGNING A HYDRAULIC OBJECT OF A DRY RESERVOIR

Jiří Skokan[*,1], Aleš Dráb[1], David Duchan[1]

[*]212397@vutbr.cz
[1]Brno University of Technology, Faculty of Civil Engineering, Institute of Water Structures, Veveří 331/95, 602 00 Brno

Abstract

This article describes and compares computational and result differences in 1D and 3D hydrodynamic models, which are used for capacity assessment of flow control structures.

The paper focuses on a considered dry retention reservoir located on the Kotojedka stream near the city of Kroměříž, Czech Republic. Based on project documentation, a detailed 1D steady hydrodynamic model using functions of Microsoft Excel and its native VBA language was created for the functional object. The parameters of the functional object were optimized based on the results of the 1D model.

During the 1D analysis, some uncertainties occurred which cannot be addressed using standard or even more complex hydraulic analytical methods, such as formation and course of hydraulic jump, manifestation of overflow and bottom inlet submergence and water surface elevation profile in apron. Experimental physical model research was not undertaken in this case due to the high cost of the model relative to its lower significance compared to other, much larger water structures. Therefore a 3D steady hydrodynamic model could bring the required solution in this case and provide the basis for object parameters optimisation. A 3D model was created using Flow – 3D software.

The results were compared on a series of Q_N flow rates from Q_{10} to Q_{10000}, where Q_N represents the discharge with a repetition period of once in every N years.

Keywords

Functional object, 1D model, 3D model, dam structure, rating curve

1 INTRODUCTION

This paper deals with flow control structures of small water reservoirs and respective dry retention reservoirs A small water reservoir is an earth-filled structure, with the limit parameters of the reservoir volume to the level of the controllable area not more than 2 million m^3 and the maximum depth of the reservoir which does not exceed 9 m.

The paper focuses on a considered dry retention reservoir located on the Kotojedka stream near the city

Water structure's flow control objects' capacity calculations greatly influence their design parameters and vice versa. The most common methods for capacity determination of flow control structures are based on 1D analytical methods. Their strength lies, compared to 3D models, in their simplified governing equations that could be solved analytically in most cases with low computational power, without aimed software and low time costs. However, these simplified methods cannot describe phenomena typical for 3D flow and their influence is often estimated in a single parameter, typically Manning's roughness coefficient, kinematic energy coefficient, etc. This estimation could lead, in a turbulent rapidly changing flow direction, to pre-measuring the design parameters of an object at best or to a threat to the safety of the hydraulic structure.

In the current state, 1D numerical models or analytical approaches are used for the design of the flow control structures [1], [2]. For less important structures, the design ends by a simplified hydraulic solution and the results are reflected in the final project documentation. For major structures, a physical modelling approach is used. Their main advantage is their predictive ability and accuracy when using a suitable model scale. The disadvantages are evident in their acquisition costs, workspace costs and limited use once the designs and project documentation are complete. A modern approach involves the use of 3D printing, which aims to reduce the cost of the model, but requires the creation of a 3D model of the project documentation or BIM and relatively high material costs. For larger objects, it is necessary to print the object in parts and complete the construction on-site in a hydraulic laboratory [3], [4]. 3D numerical modelling allows the user to simulate real flow with certain accepted simplifications. Even without calibrated data, an experienced user can set up and run the model so that the results

DOI 10.13164/juniorstav.2024.24010

are of better quality than from a 1D model. A physical model is not equal to a 3D numerical model without proper calibration and verification, but it competes very well with the operation and implementation costs and provides a good estimate of the flow characteristics that may occur in a water structure that cannot be resolved by 1D models [5], [6], [7].

This paper provides a comparison between 1D and 3D results, time costs and estimation differences. The results include computed rating curves through the bottom outlet and over weirs, water level elevation profile through the functional object and location and analysis of a hydraulic jump.

2 METHODOLOGY

This chapter introduces:

- Description of the designed object,
- the governing equations of the 1D model, the flow parameters settings and the flow diagram,
- 3D model settings,
- Methods for comparison of results.

Description of the designed object

It is a dry retention reservoir with a maximum volume of 1.6 million m^3 of water. The earthfill dam has a maximum height of 3 m. There is a road 6.5 m wide on the dam and the total width of the dam crest is 9.5 m. The dam head has a total length of 840 m, only a smaller part of 120 m was used for the actual calculations.

A concrete object with one rectangular bottom inlet opening (4.5×1.8 m^2) was designed, the inlet is closed with a gate, e.g. for inspection, repair, and test filling. The bottom inlet gate was not expected to be manipulated for controlled outflow from the reservoir. The safety spillway is of the side-channel type with a weir length of 2×36 m. The weirs are designed as semicircular with a radius of 0.5 m. The length of the apron is 61 m and the total length of the functional object is 81 m. Energy discharge of the flow is carried out throughthe stilling pool with a depth of 1 m and a length of 20 m. Fig. 1 shows a 3D visualisation model of the object. Figs. 2 to 4 show the selected cross-section and profiles of the object.

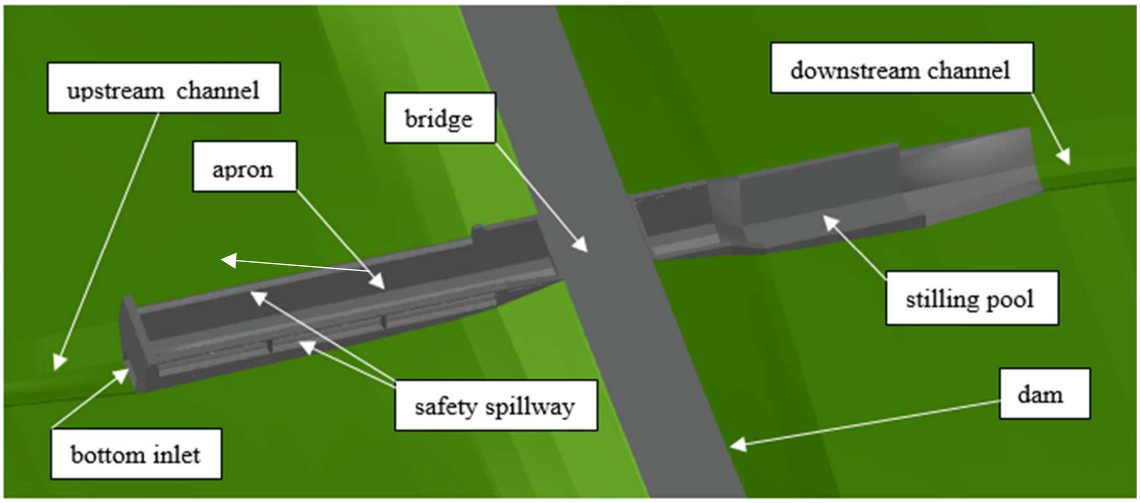

Fig. 1 3D visualisation of the designed object.

DOI 10.13164/juniorstav.2024.24010

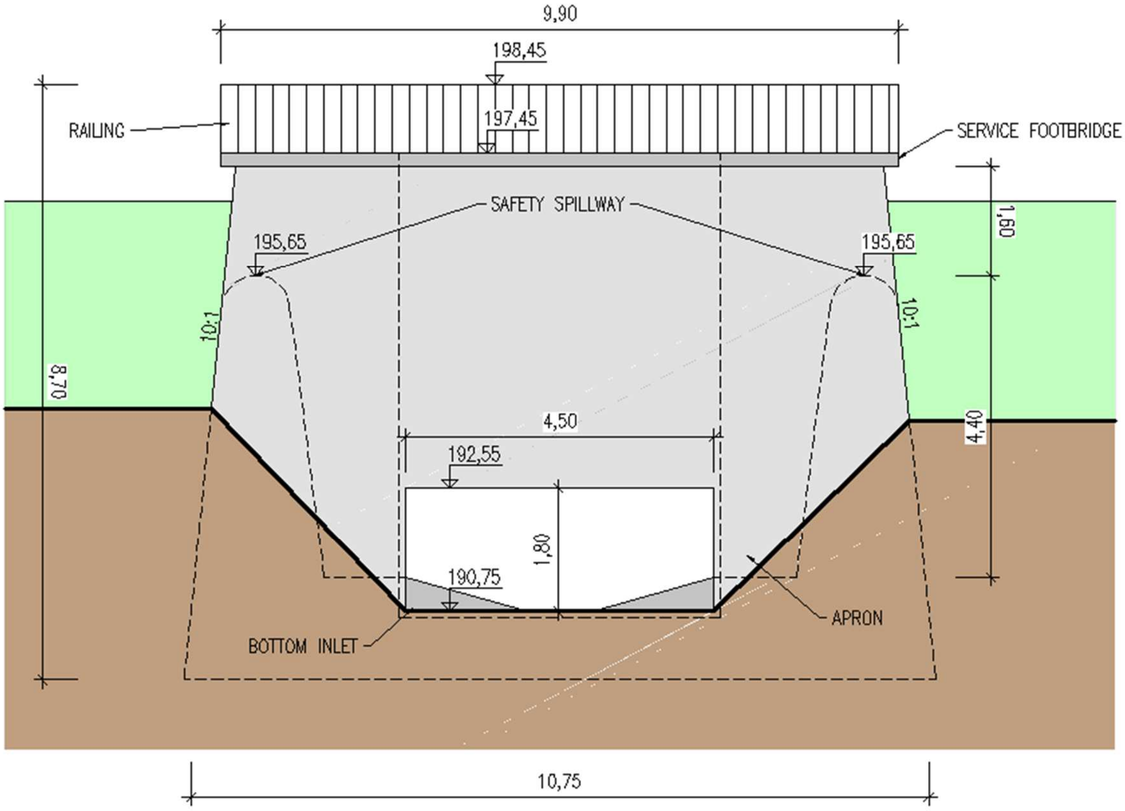

Fig. 2 View of the bottom inlet and the apron.

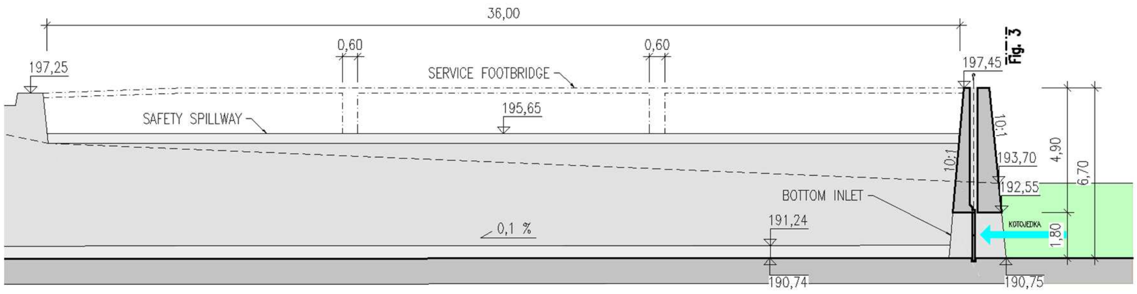

Fig. 3 Profile of the apron.

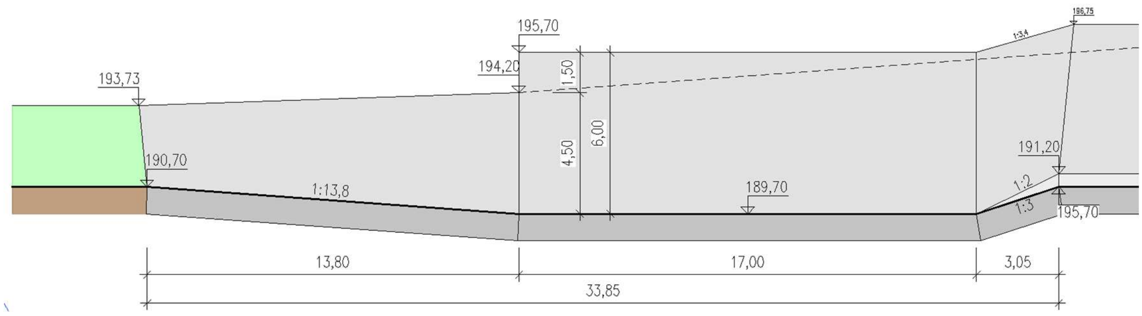

Fig. 4 Profile of the stilling pool.

1D model

For the 1D solution of the apron, 1D steady nonuniform governing equations were selected in the form of Bernoulli's equation with atmospheric pressure (1):

DOI 10.13164/juniorstav.2024.24010

$$h_1 + \frac{\alpha v_1^2}{2g} + \frac{p_1}{\rho g} = h_2 + \frac{\alpha v_2^2}{2g} + \frac{p_2}{\rho g} + \sum h_z \quad (1)$$

where h_1, h_2 is water surface elevation in profiles in m; α is kinematic energy coefficient; v_1, v_2 are average velocities in the profiles in m/s]; g is gravity constant in m/s^2; p_1, p_2 are pressures in profile in Pa; ρ is volumetric mass in kg/m^3; h_z are hydraulic losses in m [2], [3].

Flow through the bottom outlet was addressed using a 1D equation of discharge through the opening in it (2), (3), (4), (5):

- Partly submerged form,

$$Q_u = \frac{2}{3}\mu_u b\sqrt{2g}\left[\left(H + \frac{\alpha v_0^2}{2g}\right)^{\frac{3}{2}} - \left(z_1 + \frac{\alpha v_0^2}{2g}\right)^{\frac{3}{2}}\right] \quad (2)$$

$$Q_s = \mu_s a_s b\sqrt{2g\left(H + \frac{\alpha v_0^2}{2g}\right)} \quad (3)$$

$$Q_{us} = Q_u + Q_s \quad (4)$$

where Q_u is volume flow rate through the outlet‘s unsubmerged part in m^3/s; Q_s is the volume flow rate through outlet’s submerged part in m^3/s; μ_u is unsubmerged discharge coefficient; μ_s is submerged discharge coefficient; b is outlet’s width in m; H is vertical distance between highwater and tailwater in m; v_0 is mean inflow velocity in m/s; z_1 is vertical distance between highwater and inlet face in m; a_s is the height of inlet‘s submerged part in m; Q_{us} is total volume flow rate through inlet in m^3/s. [2], [3]

- Submerged form,

$$Q_{su} = \mu_{su} ab\sqrt{2g\left(H + \frac{\alpha v_0^2}{2g}\right)} \quad (5)$$

where Q_{su} is volume flow rate through submerged outlet in m^3/s; μ_s is submerged discharge coefficient; a is the height of the inlet in m; b is the outlet’s width in m. [2], [3]

Weir overflow was addressed using the weir equation (6):

$$Q_w = mb_0\sigma_z\sqrt{2g}\left(h_p + \frac{\alpha v_0^2}{2g}\right)^{\frac{3}{2}} \quad (6)$$

where Q_w is volume flow rate over weir in m^3/s; m is discharge coefficient; σ_z is submergence coefficient; h_p is overflow height in m. [2], [3]

A general equation of hydraulic jump was used for designing a hydraulic jump and sequent depths in the stilling pool (7):

$$\frac{\beta Q^2}{gS_2} + z_2 S_2 = \frac{\beta Q^2}{gS_1} + z_1 S_1 \quad (7)$$

where β is Boussinesq’s constant; Q is volume flow rate in m^3/s; z_1, z_2 are centres of gravity in the addressed profiles in m; S_1, S_2 is cross section’s flow area in m^2 [2], [3].

These equations, except the hydraulic jump design, were programmed in Excel and its VBA language, the resulting solution has the following flow chart (Fig. 5):

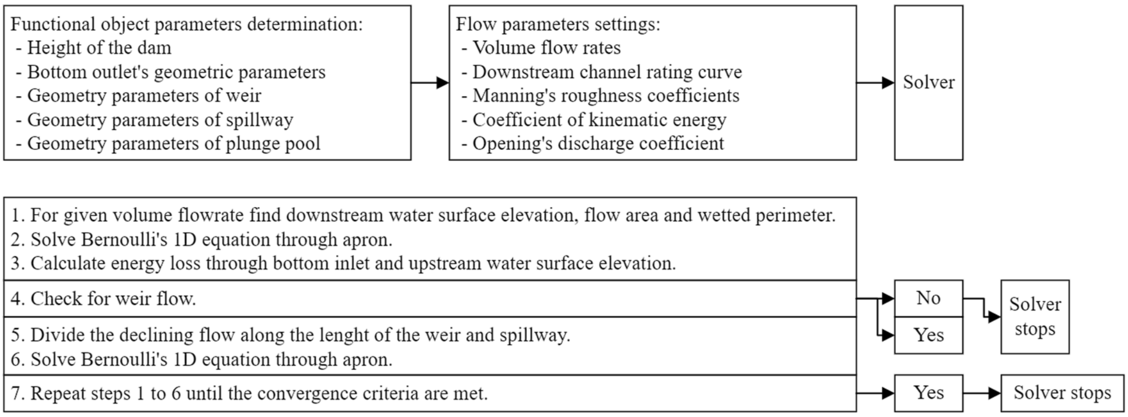

Fig. 5 1D model solution flow chart.

Where the convergence criteria are: the sum of the computed volume flow rate through the bottom outlet and weir must be equal to the input volume flow rate (8):

$$Q_{bo} + Q_w = Q_{input} \tag{8}$$

where Q_{bo} is volume flow rate through bottom outlet in m^3/s; Q_w is volume flow rate over weir in m^3/s; Q_{input} is the volume flow rate in downstream boundary conditions in m^3/s.

3D numerical model

The hydrodynamic issue was processes using Flow-3D software, which is a general-purpose computational fluid dynamics software which can carry a wide variety of fluid flows. In this case it was used to address the 3D hydrodynamic issue to determine the capacity and rating curve of a water structure functional object.

This paper does not have the capacity for a detailed description of the governing equations, so it is suggested to the readers interested to read the software manual, where the theory is well explained [8].

A .stl file which contains the created 3D object as an enclosed volume inside a triangulated surface was generated after the creation of the functional object and the adjacent dam‘s 3D model (Fig. 1), see Fig. 6.

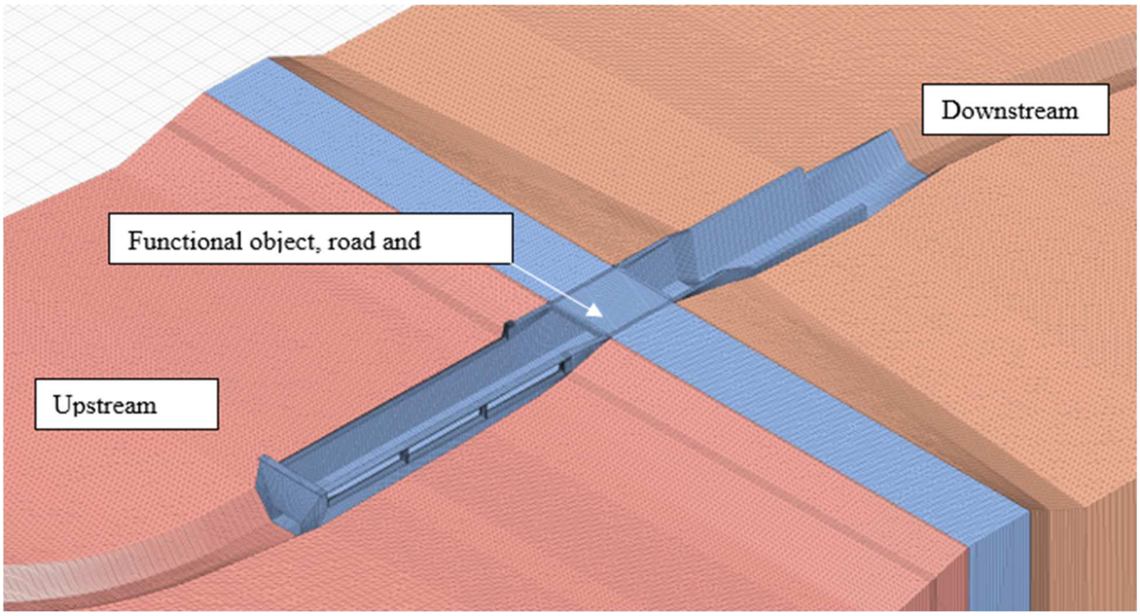

Fig. 6 Object visualisation as a .stl file.

As you can see, three separate *.stl objects were created (distinguished by colour) for the possibility of entering Manning’s roughness coefficients.

A computational mesh was generated inside the flow 3D’s user interface. Using mesh blocks, the area of interest was divided into two blocks, see Fig. 7:

- base mesh block, which contained boundary conditions. Cell size was set to 0.5 m,
- mesh block around the functional object. Cell size was set to 0.125 m.

The total number of cells was 14 million. A water surface elevation for a given volume flow rate was set as a downstream boundary condition. A water surface elevation was calculated in the 1D model for input as an upstream boundary condition and the average flow velocity perpendicular to the boundary condition plane was set.

The lack of calibrated data and chosen cell size was a reason to set two equations k–ε turbulence model. Air entrainment functions were disabled.

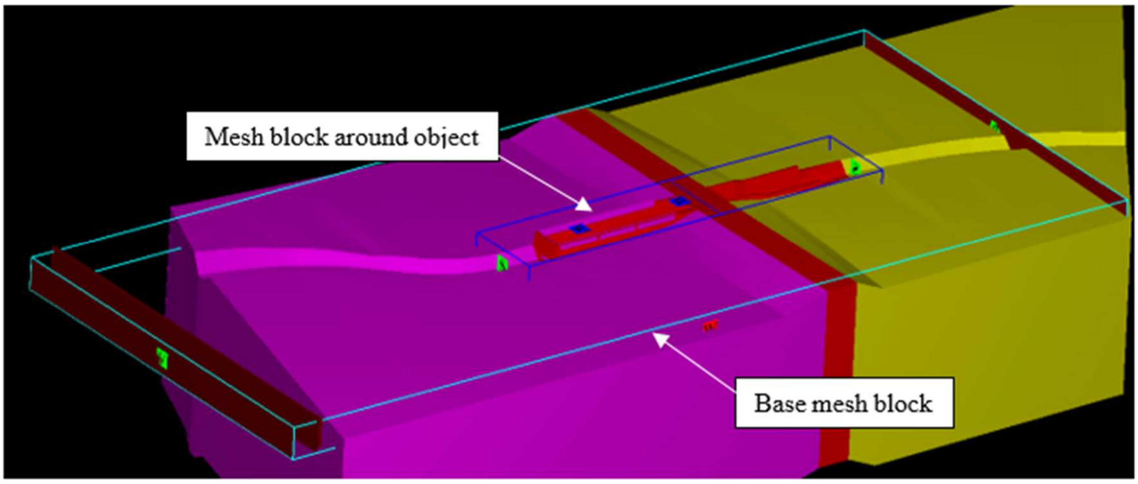

Fig. 7 Solved area inside the flow – 3D's interface.

3 RESULTS

This chapter deals with the presentation and discussion of the results.

Results were compared at three locations, see Fig. 8:

1. Bottom outlet's rating curve (Fig. 9).
2. Safety spillway rating curve (Fig. 10).
3. Water surface elevation profile through an object (Fig. 11 and Fig. 12).

Rating curves are described by the percentage difference in discharge at the same pressure or overflow height.

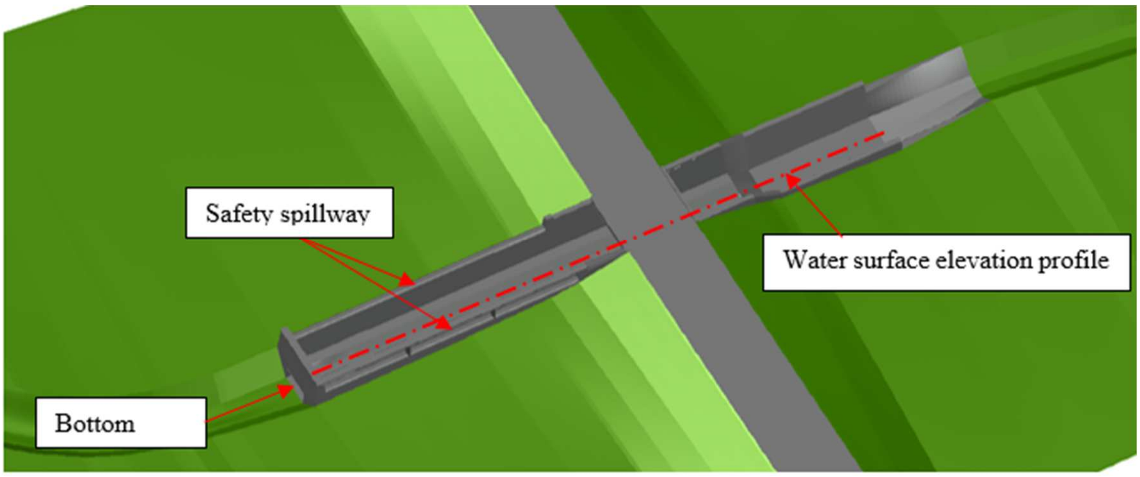

Fig. 8 Locations for the comparison of the results.

DOI 10.13164/juniorstav.2024.24010

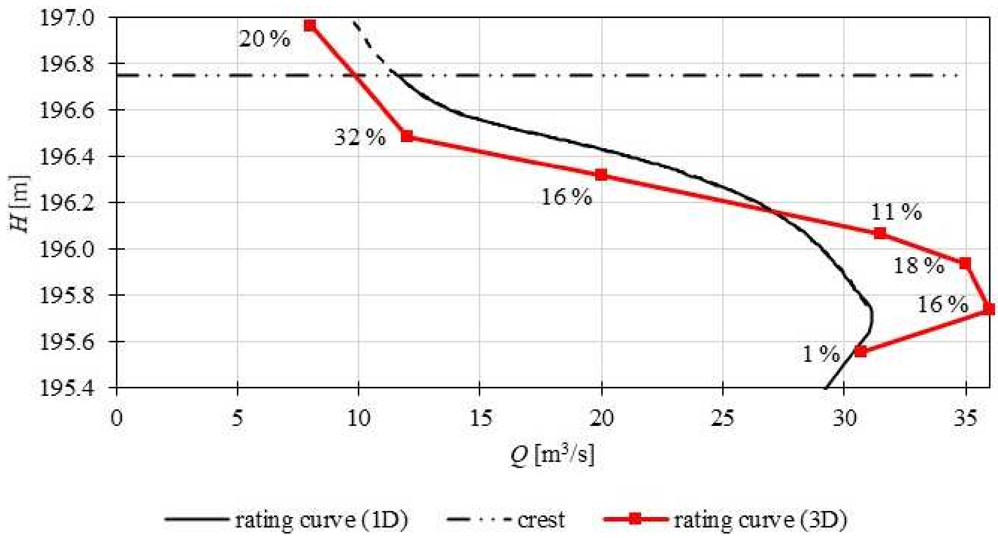

Fig. 9 Bottom inlet's rating curve.

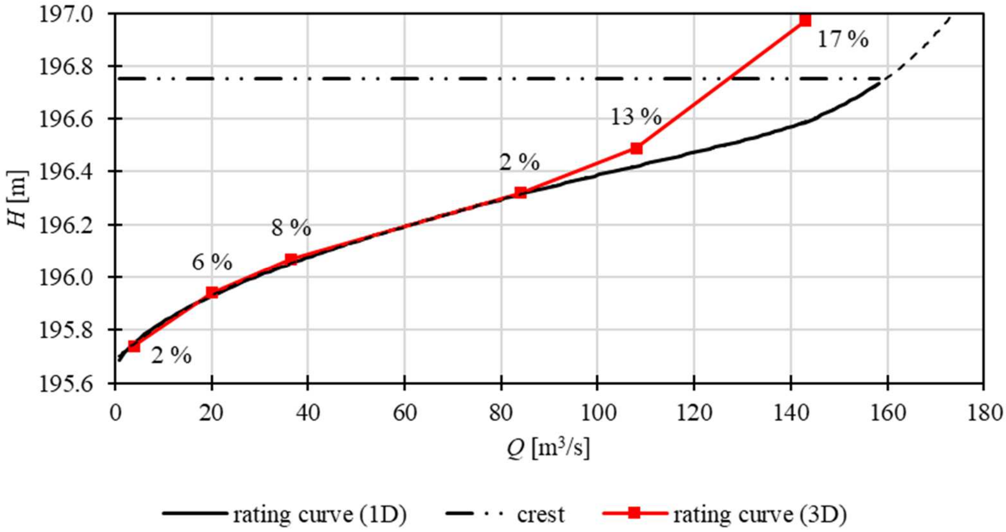

Fig. 10 Safety spillway rating curve.

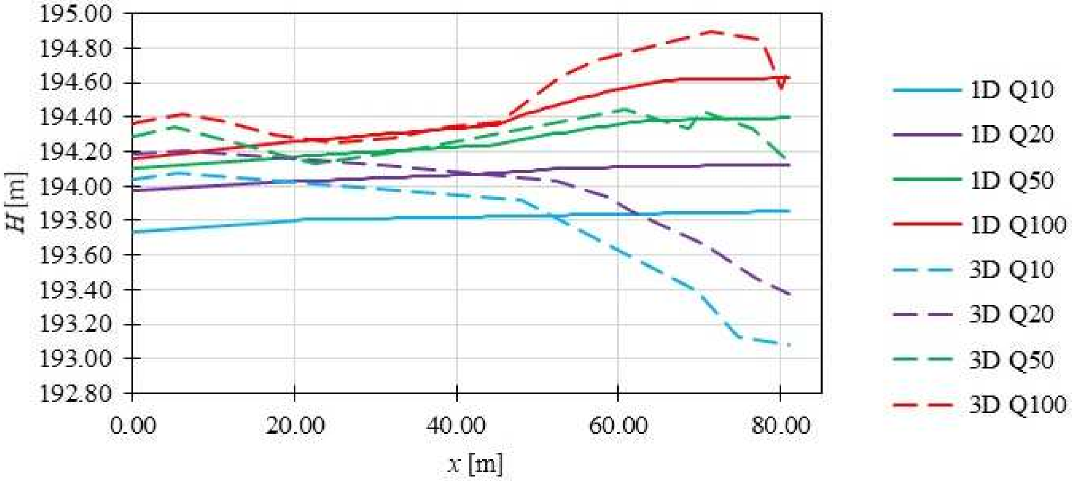

Fig. 11 Water surface elevation profile through the object for $Q_{10} – Q_{100}$.

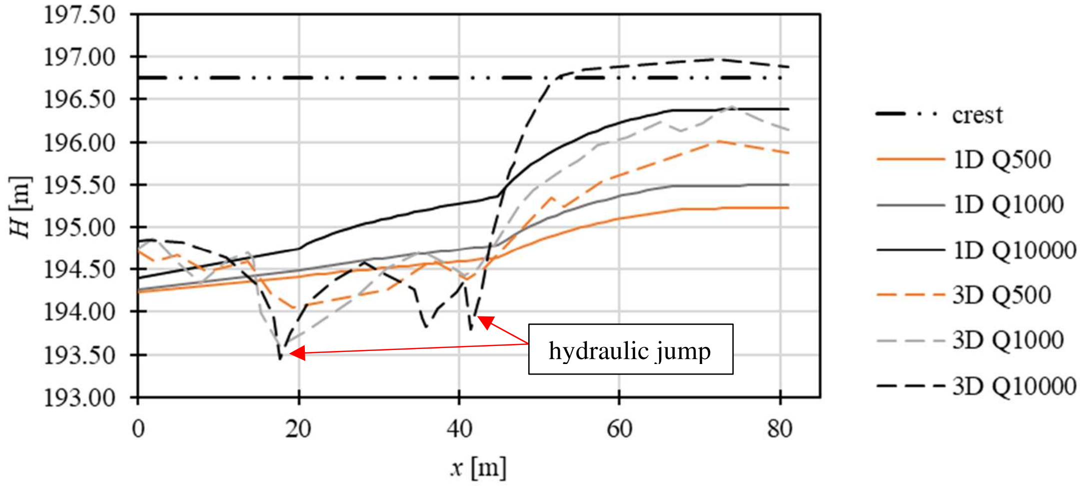

Fig. 12 Water surface elevation profile through the object for $Q_{500} – Q_{10000}$.

4 DISCUSSION

Fig. 9 shows, that the submergence effect of the bottom outlet in the 3D model manifests a greater flow rate than in the 1D case. In both cases, with the increasing submergence, the bottom outlet loses its capacity. A key finding is that in a 3D model, the maximum considered flow rate needs a pressure height greater than the height of the dam's crest, which leads to overtopping.

Safety spillway rating curves are presented in Fig. 10. The 1D and 3D models closely correspond until the submergence effect occurs. Due to the lack of information about the submerged overflow behaviour on semicircular weirs, the 1D models used a simplified method to express these effects. As can be seen, the 3D model pointed out, that the submergence from tailwater affects overflow at much lower flow rates. Lack of the capacity of the weir and apron due to the submergence effects caused that the upstream water surface elevation is higher than the dam's crest, which leads to overtopping.

As can be seen in Figs. 11 and 12, the 1D model cannot correctly describe all the phenomena occurring through the object's apron and stilling pool. 3D model results showed that a hydraulic jump occurred in the different stationing of the apron in the case of flow Q_{500} and higher. The problem arises when such phenomena as a hydraulic jump are created in places with strictly supercritical or subcritical flow because it could negatively affect flow capacity, which in the case of flow $Q_{10\,000}$ leads to crest overtopping. 1D model results showed subcritical flow along the entire length of the apron, therefore the hydraulic jump cannot be addresses using a general 1D solution of sequent depths not to occur.

The 3D hydraulic model addressed the combination of the flow through the bottom inlet and the safety spillway, which is a hydraulically very complex issue. In the 1D model, the flow complexity tried to be solved by combining the hydraulic calculations for each part of the object into one solution.

Completion times for one addressed state for the 1D model was 3.5 seconds (0.0009 hours), and the 3D model took 72 hours to dealt with one complete calculation. Such a difference in favour of the 1D model allowed the user to solve in one run 172 steady states (in total of 10 minutes) and thus create rating curves and profiles for a full range of flow rates. 3D model dealt with one steady state for approximately 72 hours, which allowed to test only a narrower range of flow rates.

5 CONCLUSIONS

This paper compared the results of the 1D and 3D modelling approach in the form of the water surface elevation profile in the object and the rating curves of the bottom outlet and weirs, which are currently used to design the capacity parameters of water structures.

The results show that the 1D model provides fast results based on which it is possible to make operational adjustments to the object parameters, but it is not able to describe the phenomena for 3D flow, in which uncertainties that threaten the safety of the designed object may occur.

DOI 10.13164/juniorstav.2024.24010

For flows up to Q_{500}, the differences in the established rating curves are minimal and the differences in the water surface elevation profile in the object are not at the safety limit of its capacity.

For flows greater than Q_{500}, uncertainties that the 1D model is not able to capture the reality began to manifest themselves, particularly safety spillway's overflow submergence, transitions between supercritical and subcritical flow in the object, and izs capacity, which in the case of flow $Q_{10\,000}$ leads in a 3D model to the dam's crest overtopping.

The best results would be provided by the physical model research, based on which calibration of 1D and 3D model parameters would be performed. In this case, however, the lower significance of the structure relative to the high cost of implementing the physical model does not allow creating it for the research. The 3D numerical model at least provides a coarser overview of the conditions that can occur in the structure and highlights the uncertainties that can lead to a breach to the water structure and the occurrence of a special flood.

Acknowledgements

This article was elaborated with the support of the project FAST-S-23-8233 Sensitivity analysis of selected input parameters in water flow numerical modelling.

References

[1] JAMES, C S. Hydraulic structures. 1. Switzerland: Springer Cham, 2020. ISBN 978-3-030-34085-8

[2] CHEN, Shenghong. Hydraulic structures. 1. Heidelberg: Springer-Verlag, [2015]. ISBN 978-3-662-47330-6

[3] KASIMOV, J.A.; KAMILOV, A.I.; MUSTAFOYEVA, D.A. and NASRITDINOVA, U.A. Building a 3D model of hydraulic structures using BIM technology. Online. E3S Web of Conferences. 2023, y. 402, p. 5021, [accessed 2023-10-09]. ISSN 2555-0403. Available at: https://doi.org/10.1051/e3sconf/202340205021

[4] OERTEL, Mario and SHEN, Xiaoyang. 3D Printing Technique for Experimental Modeling of Hydraulic Structures: Exemplary Scaled Weir Models. Online. Water (Basel). 2022, y. 14, n. 14, p. 2153. ISSN 2073-4441. Available from: https://doi.org/10.3390/w14142153. [cit. 2023-10-09]

[5] BAYÓN BARRACHINA, Arnau. Numerical analysis of air-water flows in hydraulic structures using computational fluid dynamics (CFD). 2018. PhD Thesis. Universitat Politècnica de València

[6] KIM, B.-J.; HWANG, J.-H.; KIM, B. FLOW-3D Model Development for the Analysis of the Flow Characteristics of Downstream Hydraulic Structures. Sustainability 2022, 14, 10493. https://doi.org/10.3390/su141710493

[7] NGUYEN, Van Thinh. 3D numerical simulation of free surface flows over hydraulic structures in natural channels and rivers. Applied Mathematical Modelling. 2015, roč. 39, č. 20, s. Pages 6285-6306. ISSN 0307-904X

[8] Flow Science, Inc., Santa Fe, NM, USA. FLOW-3D® Version 2023R1 Users Manual (2023) [Online]. Accessed: June 6, 2023. Available at: https://www.flow3d.com/